

NEW RESULTS ON THE WATERLESS AREA, WADI
EL-NATRUN DEPRESSION.

A.,GH., HASSANEEN*, H.,M., EL-SHAYEB** & M.,A., KHALIL*

* National Research Institute of Astronomy and Geophysics

** Geology Department, Faculty of Science, Menoufia University

ABSTRACT

The main aim of the present study is to re-evaluate the groundwater potentiality in the area previously called waterless area at Wadi El-Natrun depression. Waterless area was studied by Shata, et.al.1962. He stated that , the waterless area is interpreted geologically as a lacustrine deposits Fig (1). Also all boreholes in this area are non-productive wells Fig (2).

The geoelectric survey in this area and its vicinities indicates that, there are three fault systems forming a small structural basin where, the lacustrine deposits are consequently accumulated with a depth of about 100m.. Also, the Pliocene water bearing formation is found beneath these deposits . So, we can call this area as a deep water area and the non-productive wells should be reproduced by increasing its depth to more than 100m..

INTRODUCTION

At the outset , it is important to refer to the location of Wadi El-Natrun depression. Wadi El-Natrun depression is located between Latitudes $30^{\circ} 15' N$ and $30^{\circ} 30' N$ and Longitudes $30^{\circ} 00' E$ and

A.,GH., HASSANEEN*, H.,M., EL-SHAYEB** & M.,A., KHALIL*

30° 30' E, covering an area of about 500 sq. km. It is characterized by the presence of a large number of salt water lakes, which are distributed in the main depression. The lowest point of this depression is about 23m. bsl.

The target of the present paper is to illustrate the applicability and limitations of the resistivity method in identifying the groundwater potentialities in the study area.

GEOLOGIC CONDITION

The shallow geological succession of the area under investigation was studied by El-Fayomi, 1964. The study area is considered as the type locality of Wadi El-Natron Formation Fig.(3), which is considered as the main water bearing formation in the study area, and can be illustrated as follows :

Wadi El-Natron Formation:-

It is composed of clays which is overlain by argillaceous sands and limestone beds. It is subdivided into two members:-

1-El-Muluk Member : It is about 30m. thick composed of pyretic and gypseous sands , dark clay alternating with sandy beds.

2- Beni-Salama Member : It is about 40m. thick, composed of fossiliferous argillaceous sand in the upper part of 30m. but the lower part is unfossiliferous sands.

Structurally, Wadi El-Natron depression is a complicated structure feature According to Sanad, 1975. which consists of folds, faults, grabens and basins. There are two fold systems, the first is the buried NE-SW (Syrian arc fold system) which is probably related to the Late Mesozoic-Early Tertiary laramid

deformation phase. The second is the NW-SE (Clysmic fold system). It is mostly related to the Neogene Syrian movement.

Wadi El-Natron and Wadi El-Farigh anticlines are belonging to the second fold system . So that, Wadi El-Natron depression consists structurally of a monocline dissected by a three sets of faults, as follows

- 1- NW-SE (Clysmic system).
- 2-NE-SW (Aqaba trend).
- 3-E-W (Tethyan system).

METHODOLOGY AND INSTRUMENTS

The study area was measured and covered by 60 VESes forming a grid. The spacing is ranging from 300 to 500m. (Fig, 4). Vertical electrical sounding is considered as one of the most suitable methods for underground water exploration. The sounding was carried out using Schlumberger array with AB/2 ranging from 1m. to 300m., and MN ranging from 0.4m. to 40m.

All measurements were occupied by 60 watts D.C resistivity meter model GGA31 (Bdensewerk production - Germany) with a microprocessor and RS-232 interface . Zohdy (1989) software is devoted to the task of calculating the number of layers, their thickness and their true resistivities.

DISCUSSION

The field data in the form of apparent resistivity was interpreted and discussed both qualitatively and quantitatively. Qualitative interpretation is carried out in the form of iso-apparent resistivity contour maps and pseudo-resistivity sections to show both the vertical and horizontal variations in ohmic values and their geological contribution.

(1)- QUALITATIVE INTERPRETATION :-

(A)-Iso-apparent resistivity contour maps:

This type of maps is established by contouring the resistivity values of all stations at the same apparent depth expressed by $(AB/2)$ to show the horizontal variation in resistivity. Five maps are prepared at $AB/2= 10m, 60m, 100m, 200m$ and $300m$. The examination of these maps (Figs.5,6,7,8 and 9) shows that :-

- 1)- Figs. 5 and 6 at $AB/2 = 10m.$ and $60m.$ are characterized by high resistivity values in the middle and eastern parts of the area with moderate values in between. The abrupt changes in resistivity values reflect the presence of an inferred fault system such as F1 and F2 in the area. Also it reflects the dryness of this geoelectric zone . So that it is corresponding to the Pleistocene dry sands and gravels.
- 2)- Figs. 7 and 8 at $AB/2 =100 m.$ and $200 m.$ are characterized by homogeneous distribution of moderate to low resistivity values . These ohmic values are corresponding to the Pliocene water bearing formation.
- 3)- Fig. 9 at $AB/2=300m.$ is characterized by homogenous distribution of low to very low resistivity values, which is corresponding to the Mio-Pliocene impervious clay bed and the water bearing formation.

The previous iso-apparent resistivity contour maps can be classified into three geoelectric zones. The first zone begins from the ground surface to the apparent depth of $AB/2=60m.$ (true depth $\sim 24m.$). It is corresponding to the Pleistocene dry sands and gravels . The second zone from $AB/2=60m.$ to $AB/2=200m.$ with a true depth of about $80m.$. It is corresponding to the Pliocene water bearing formation. The third zone, from a true depth of about $80 m.$ to undetected depth, is corresponding to the water bearing formation

and the Mio-Pliocene impervious clay bed .

(B)-Pseudo-Resistivity Sections:

1- Pseudo-Resistivity Section (A-A'):-

This section Fig.(10) trends in NE-SW direction, passing through VESes 29, 30, 31, 32, 33 and 34. The general style refers to high resistivity values near the surface at VESes 31 and 33 and in the middle of VES 31, then gradually decrease to moderate and low values in the other parts of this section. This variation in the resistivity values reflects the lithologic variation along this profile.

2- Pseudo-Resistivity Section (B-B'):-

This section Fig.(11) trends in NE-SW direction, passing through VESes 35, 36, 37, 38, 39 and 40. The resistivity values are characterized by very high to high values at VESes 40, 36 and 37 . These high resistivity values decrease gradually at the area in between to low and middle resistivity values. This large change in the resistivity values may indicate an inferred fault system between VES 40 and 39.

3- Pseudo-Resistivity Section (C-C') :-

This section Fig.(12) trends in NW-SE direction, passing through VESes 2, 8, 14, 21, 24, 30, 36 and 42. The examination of this section shows that, there are high resistivity values at VESes 42, 36 and 30 and at the surface of VESes 14 and 21. These high values decrease suddenly to very low resistivity values at VESes 2 and 8 and at deep depths in VESes 14, 21 and 24. This sudden change in resistivity values may refer to the presence of an inferred fault system between VESes 21 and 24.

4- Pseudo-Resistivity Section (D-D'):-

This section Fig.(13) is trending in NW -SE direction, passing through VESes 3, 9, 15, 16, 25, 31, 37 and 59. It is characterized by very high to high resistivity values at VESes 16, 25, 31, 37 and 59. It decreases gradually to low resistivity values in deep sites and in the direction to VES 3 and at the surface of VES 15. This variation in resistivity values refers to the variation in lithology.

(2)- QUANTITATIVE INTERPRETATION :-

The apparent resistivity data were converted into its true thickness and resistivity using Zohdy,(1989) software.

(A)- Electric and Geologic Cross - Sections (A-A') :-

These sections Figs.(14) and (15) are constructed depending on the interpretation of the VESes 29, 30, 31, 32, 33 and 34, in the NE-SW direction. It is characterized by a number of geoelectric layers ranging from 4 to 5. The left side of this section, which contains VESes 29, 30, 31, and 32 and represents the downthrow of the fault can be interpreted as follows:

The first geoelectric layer in the profile, as shown at VES 29, is characterized by low resistivity value of 6 Ohm-m. It represents an extension of a clay bed.

The second geoelectric layer in the profile, as shown at VESes 29 and 30 is characterized by moderate resistivity values ranging from 27 to 39 ohm-m. Its thickness varies from 25 to 31 m. This layer is corresponding to the Recent aquifer that consists of silt deposits of the Nile Delta as shown in the corresponding geologic cross-section Fig.(15).

The third geoelectric layer in the profile, as shown at VESes 29, 30, 31 and 32 is characterized by high resistivity values ranging from 170 to 258 ohm-m.

with thickness of 46 to 90 m. It represents the Sub-Recent lacustrine deposits of Pleistocene period.

The fourth geoelectric layer in the profile as shown at VESes 30, 31 and 32 is characterized by moderate resistivity values ranging from 35 to 99. It represents the Pliocene aquifer.

The fifth geoelectric layer as shown at VES 32 is characterized by a low resistivity value of 16 ohm-m. It represents the Mio-Pliocene clay bed.

With respect to VESes 33 and 34, that located in the upthrown side of the fault, the succession is as follows :

The first geoelectric layer in the profile is present at VES 34 only. It is a thin bed of moderate and low resistivity values. It represents a clayey or loamy layer with 14 Ohm-m resistivity and a thickness of 5 m.

The second geoelectric layer in the profile, as shown at VESes 33 and 34, is characterized by moderate resistivity values ranging from 32 to 34 ohm-m , with a thickness ranging from 3 to 16m. It represents the extension of the Pliocene aquifer, that is present in the downthrown side of the fault.

The third geoelectric layer in the profile is characterized by low resistivity values ranging from 3 to 9 ohm-m with a large thickness of the Mio-Pliocene clay bed as shown in Fig.(15).

The fourth geoelectric layer appears at VES 34 only. It has a resistivity of 55 ohm-m. It represents the top of the Miocene aquifer .

It is clear that, the three aquifers which are distributed in the study area and its vicinities are represented in this section . The Recent aquifer is found under VESes 29 and 30 at shallow depth. The Pliocene aquifer is found under VESes 29, 30, 31 and 32 at a larger depth than the first , but it is found under VESes 33 and 34 at very shallow depth. The third aquifer is found under

VES34 only . It represents the deep Miocene aquifer as shown in the geologic cross-section Fig.(15).

This section is affected by two inferred fault systems forming a grabenal structural feature. So that , the cycle of deposition is different from one part to another around the fault plane.

(B)- Electric and Geologic Cross - Sections (B-B') :-

These sections Figs.(16) and (17) are constructed depending on the interpretation of the VESes 35, 36, 37, 38, 39 and 40, in the NE-SW direction. They are characterized by a number of geoelectric layers ranging from 2 to 3 , which are represented as follows :

The first geoelectric layer in the profile , as shown at VESes 35, 36, 37 and 40 is characterized by high resistivity values ranging from 149 to 661 ohm-m. with a thickness ranging from 37 to 100 m. It represents the dry lacustrine deposits at VESes 35, 36 and 37, and the dry sands and gravels of Pleistocene Period at VES 40.

The second geoelectric layer in the profile, as shown at all VESes is characterized by moderate resistivity values ranging from 25 to 86 ohm-m. It represents the Pliocene aquifer.

The third geoelectric layer in the profile, as shown at VESes 37, 38, 39 and 40, is characterized by low resistivity values ranging from 8 to 14 ohm-m. It represents the Mio-Pliocene clay bed of El-Mekhiemen Formation.

These sections are characterized by the presence of a clay lens at VES 38 with a resistivity of 12 ohm-m. Also, there is an inferred fault system between VESes 37 and 38.

(C)- Electric and Geologic Cross - Sections (C-C') :-

These sections Figs.(18) and (19) are constructed depending on the

interpretation of the VESes 2, 8, 14, 21, 24, 30, 36 and 42 in the NW-SE direction. They are characterized by a number of geoelectric layers ranging from 2 to 3, which are represented as follows :

The first geoelectric layer in the profile, as shown at VESes 14, 21, 36 and 42, is characterized by high resistivity values ranging from 149 to 1600 ohm-m. with a thickness ranging from 5 to 99 m. It represents the surface layer and the Sub-Recent lacustrine deposits of Pleistocene Period.

The second geoelectric layer in the profile , as shown at all VESes, is characterized by middle resistivity values ranging from 21 to 99 ohm-m. It represents the Pliocene aquifer.

The third geoelectric layer in the profile, as shown at VES 42 is characterized by low resistivity values of 13 ohm-m. It represents the Mio-Pliocene impervious clay bed.

In these two cross-sections there are two features characterized by :-

- 1-A clay lens under VES 24 near to the surface and
- 2-A grabenal structural feature, that contains the lacustrine deposits in the downthrown side.

(D)- Electric and Geologic Cross - Sections (D-D') :-

These sections Figs.(20) and (21) are constructed depending on the interpretation of the VESes 3, 9, 15, 16, 25, 31, 37 and 59 in the NW-SE direction. They are characterized by a number of geoelectric layers ranging from 2 to 3, which are represented as follows :

The first geoelectric layer in the profile, as shown at VESes 16, 25, 31, 37 and 59, is characterized by high resistivity values ranging from 154 to 781 ohm-m. with a thickness ranging from 13 to 90 m. It represents the Sub-Recent lacustrine deposits of Pleistocene Period as shown in the geological

cross-section Fig.(21).

The second geoelectric layer in the profile, as shown at all VESes is characterized by moderate resistivity values ranging from 35 to 103 ohm-m. It represents the Pliocene aquifer.

The third geoelectric layer in the profile, as shown at VESes 9, 15, 37 and 59, is characterized by low resistivity values ranging from 9 to 15 ohm-m. It represents the Mio-Pliocene impervious clay bed.

These two sections are affected by a grabenal structural feature leading to the deposition of lacustrine deposits in the graben.

RESULTS

As the waterless area was interpreted geologically as a lacustrine deposits (Shata,1962), and the salines were formed by evaporation under the aridity conditions. The location of these lacustrine deposits is shown in the soil map of the study area Fig.(22). Geoelectrically the waterless area is a structural basin, that is separated from its boundaries by three inferred fault systems Fig.(23). These fault systems are classified as follows :-

1-F₁ -F'₁:- is the main dominant fault . It cuts all the study area and parallel to the extension of the lakes. The downthrown side of this fault is in the northern direction of the waterless area.

2-F₂ -F'₂ and F₃ -F'₃ :- They are two inferred fault systems terminating from the main fault F₁ -F'₁ . The downthrown side is in the direction of the waterless area.

3-F₄ -F'₄:- is a normal fault system locating inside the waterless area.

From the above discussion, the waterless area is affected by two graben faulting systems and one step faulting system. These faults are forming a structural basin, where the lacustrine deposits are accumulated in.

From the examination of the prepared geoelectric cross-sections , it can noticed that, the lacustrine deposits have a thickness ranging from about 40 to 100 m. Fig.(24) with a true resistivity ranging from 149 to 781 ohm-m Fig.(25).

From the geological and geoelectrical points of view , the previously called waterless area should be called the deepwater area where, the depth to the Pliocene aquifer reaches about 100 m. Fig.(26). This large depth to water is contributed to the large thickness of the lacustrine deposits, which overlain the Pliocene aquifer.

RECOMMENDATIONS

It becomes very clear that, there is a good probability of the production of water from this area after increasing the depth of the present wells (non-productive wells) reaching a depth not less than 100m. Logically, the deep water area can be considered as the best productive sector in the area under investigation due to its low level compared with its vicinities of the Pliocene water bearing formation as shown in the water table map Fig.(27), where the general direction of groundwater flow is in the direction of the main Wadi El-Natrun depression, with the presence of a local groundwater flow direction to the deep water area.

REFERENCES

- 1-Darwish,M.,H., (1965) : Geology and Mineralogy of the saline deposits of Wadi El-Natrun, Egypt. V.A.R. Cairo Fac. Sci. Ain-Shams Univ.
- 2-Desert Institute (1970) : Geomorphology, Geology, Hydrology, and the soils of Wadi El-Natrun-Maryut Agricultural Project. Internal report ,Cairo, Egypt, 43 pp.
- 3-El-Fayoumi, L.F.(1964) : Geology of groundwater supplies in Wadi El-

Natron area. M. Sc. Thesis Fac. of Science, Cairo Univ.

- 4-El-Shazly, E.,M., Abdel Hady, M.,A., El-Ghawaby, M.,A.and El-Kassas, A.(1975) :Geologic Interpretation of landsat Satellite Images for West Nile Delta Area. Egypt. Academy of Scientific Research and Technology, June, 1975.
- 5-Said, R., (1991) : The Geology of Egypt. Balkema publ., Rotterdam, Nether lands. 734 pp.
- 6-Sanad, S. (1973) : Geology of the area between Wadi El-Natron and the Moghra depression . Ph.D. Thesis. Fac. Sci. Assuit Univ.
- 7-Shata, A., (1953) : New Light on the structural developments of the western desert of Egypt , Bull. Inst. Desert. Egypt. 3(1), p 101-106.
- 8-Shata,A., Pavlov,M.and Saad,K.(1962) : Preliminary report on the geology ,hydrology and groundwater hydrology of Wadi El-Natron and adjacent areas. Unpublished report, Desert instiute Cairo. Egypt.
- 9-Zohdy, A.R., (1975): Automatic interpretation of schlumberger sounding curves using modified Dar Zarrouk functions, Ball.13 B-E, U. S. Geological survey.
- 10-Zohdy,A.R.(1989) : New method for automatic interpretation of Schlumberger and Wenner sounding curves, Geophysics, V-54, N. 2P. 245-253.
- 11-Zohdy, A. R., and Bisdorf, R. J.,(1989) : Programs for the automatic processing and interpretation of Schlumberger sounding curves in quick basic 4.0, Open-File Report 89-137, AB, .S. Dept. of interior, Geol. Surv.

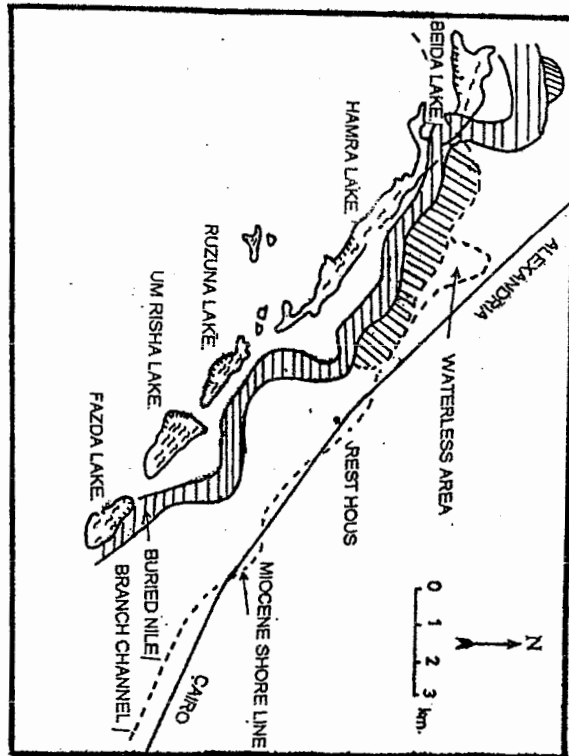


FIG.(1) : HYDROGEOLOGICAL MAP OF WADI EL NATRUN, (AFTER SHATA, 1962).

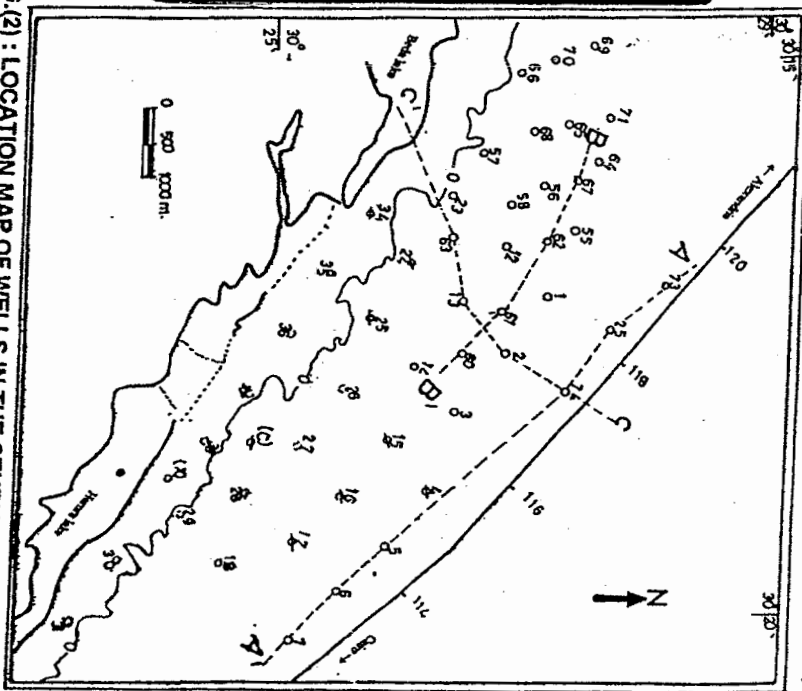


FIG.(2) : LOCATION MAP OF WELLS IN THE STUDY AREA (AFTER DESERT DEVELOPMENT AUTHORITY, 1961).

- Productive wells
- Exploratory well
- Non productive wells
- Spring
- Hydrogeologic cross section

A.,GH., HASSANEEN* H.,M., EL-SHAYEB** & M.,A., KHALIL*

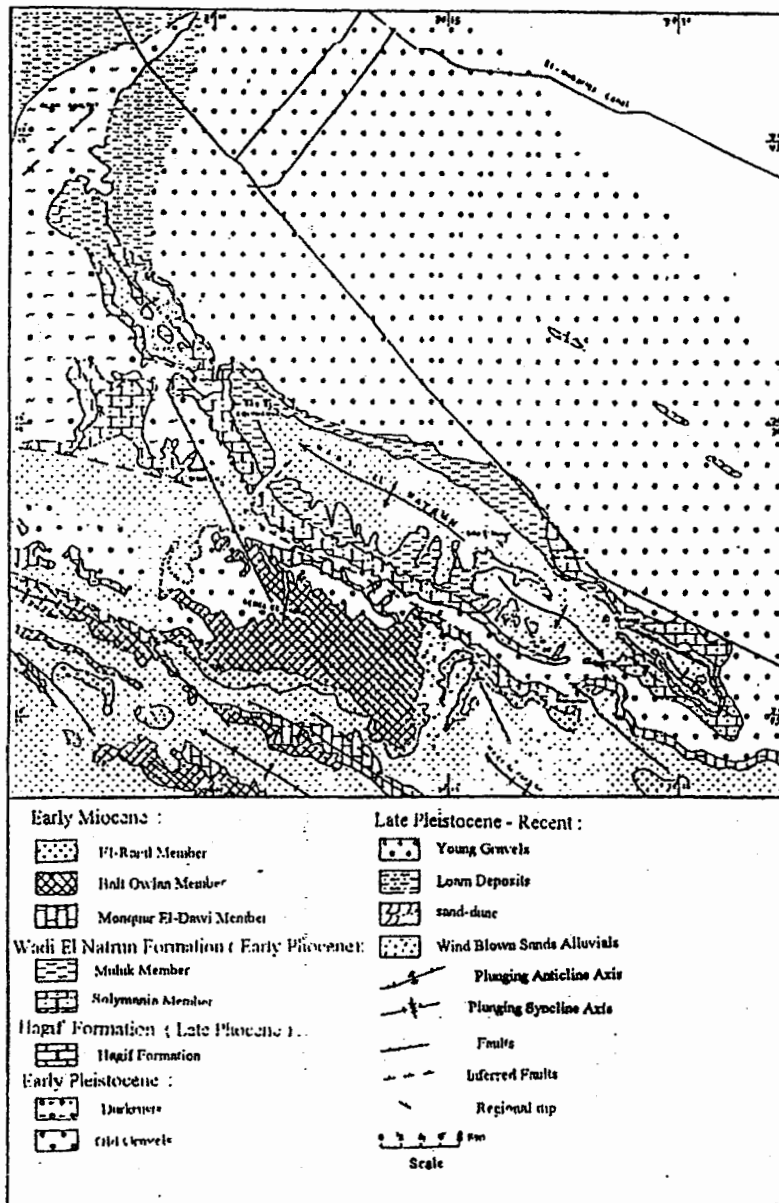


FIG.(3) : GEOLOGICAL MAP OF THE AREA WEST OF THE NILE DELTA. (after sanad ,1973) and modified

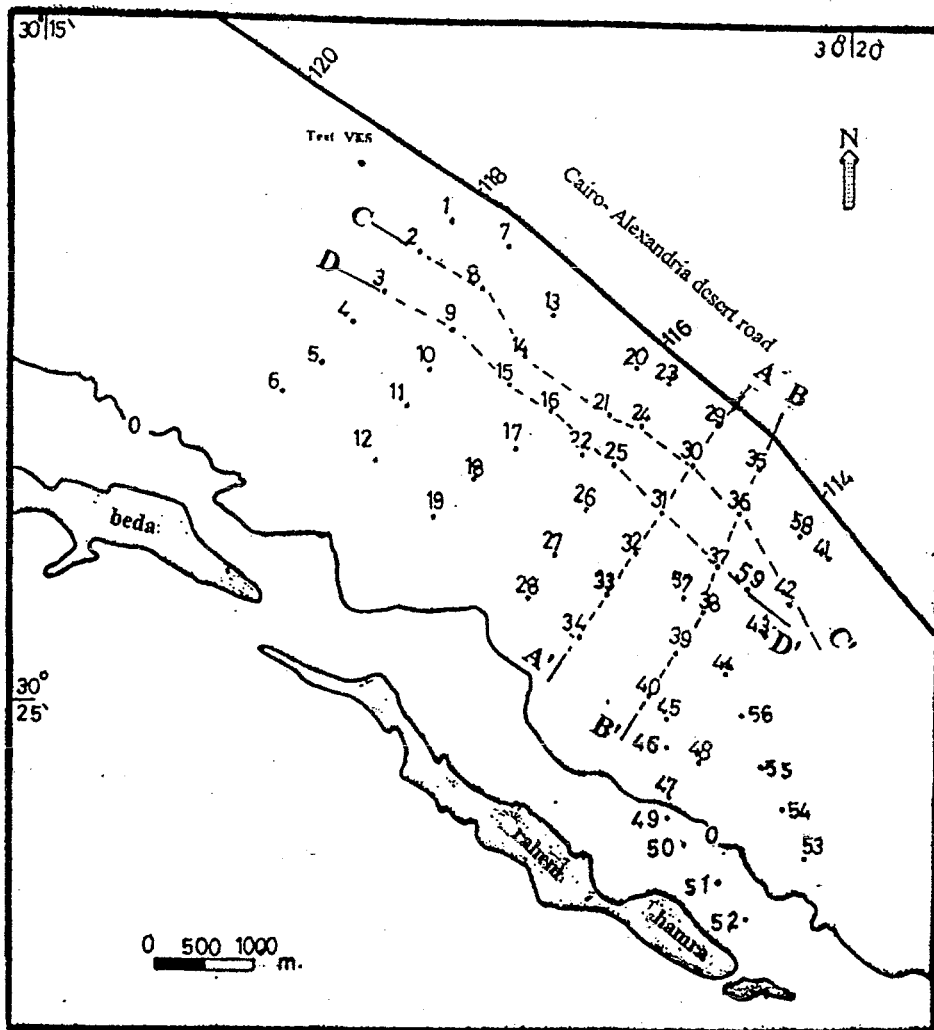


Fig.(4) locations of V.E.S stations and geoelectrical cross-sections in the study area .

● vertical electrical soundings (V.E.S)

----- Geoelectrical cross-section

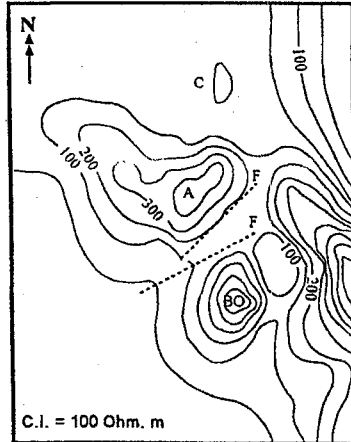


Fig. 5: Iso-Apparent Resistivity Contour Map at $AB/2 = 10m$

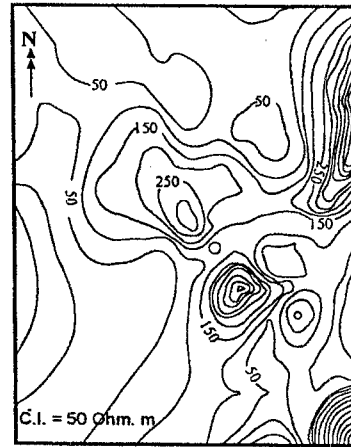


Fig. 6: Iso-Apparent Resistivity Contour Map at $AB/2 = 60m$

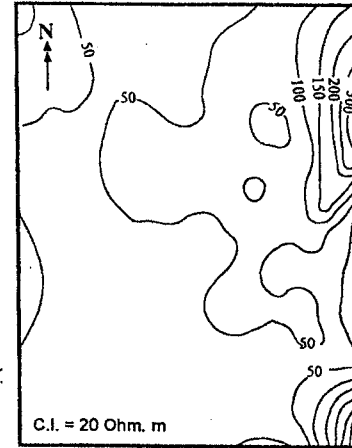


Fig. 7: Iso-Apparent Resistivity Contour Map at $AB/2 = 100m$

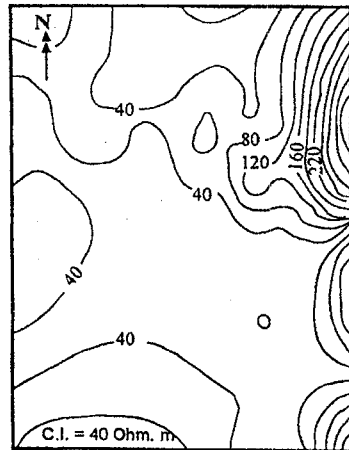


Fig. 8: Iso-Apparent Resistivity Contour Map at $AB/2 = 200m$

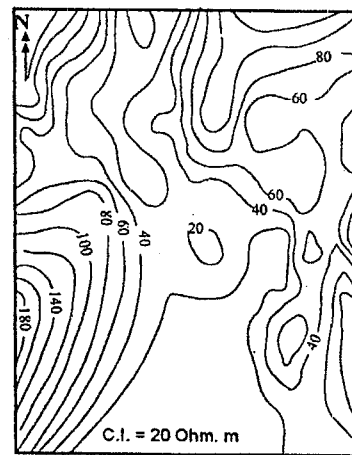


Fig. 9: Iso-Apparent Resistivity Contour Map at $AB/2 = 300m$

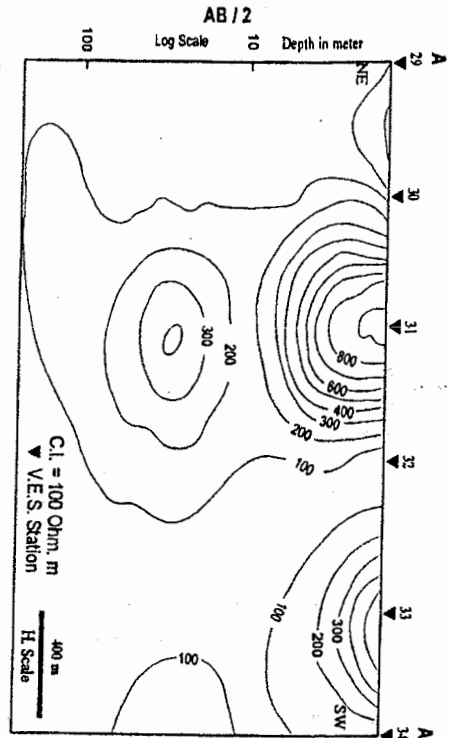


Fig. 10: Pseudo Resistivity Section (A-A')

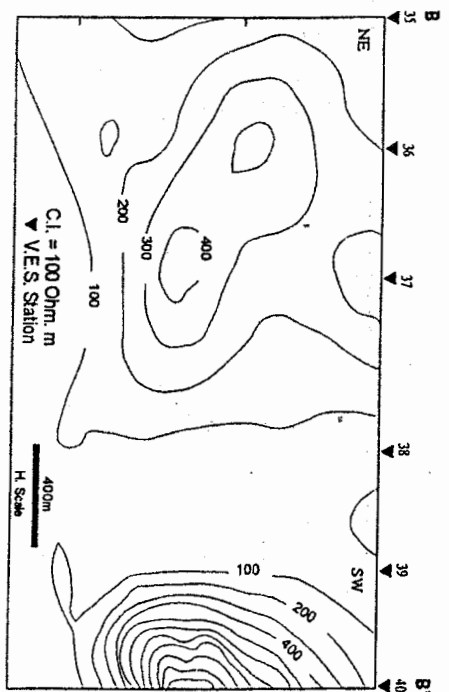


Fig. 11: Pseudo resistivity section (B-B')

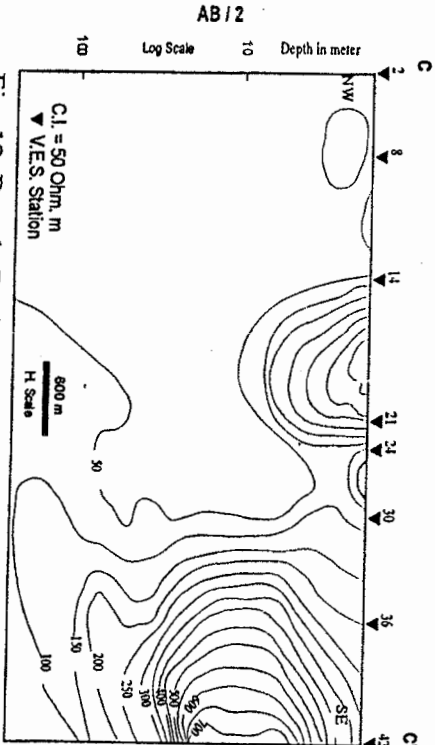


Fig. 12: Pseudo Resistivity Section (C-C')

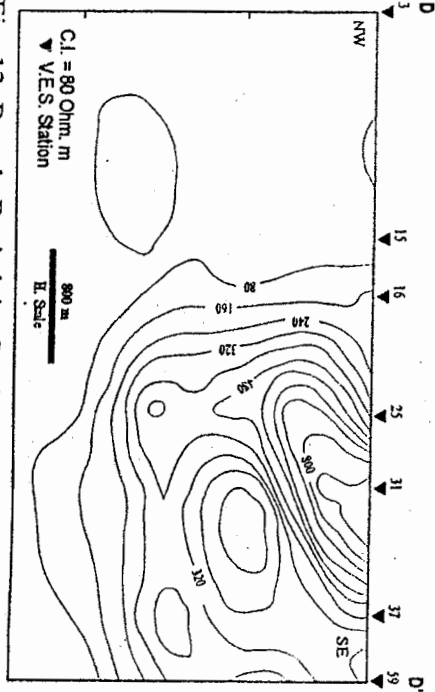


Fig. 13: Pseudo Resistivity Section (A-A')

A.,GH., HASSANEEN*, H.,M., EL-SHAYEB** & M.,A., KHALIL*

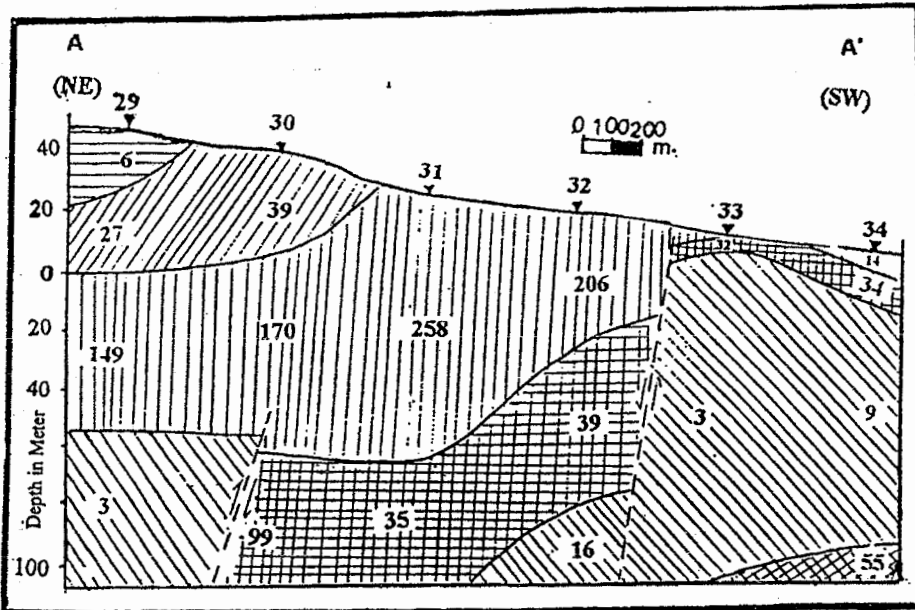


FIG.(14): ELECTRIC CROSS- SECTION (A-A').

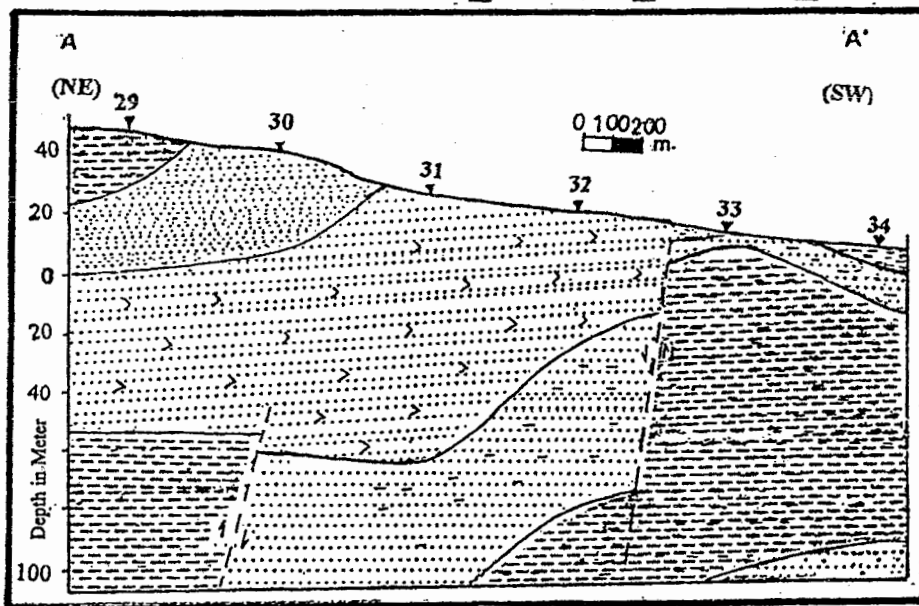


FIG.(15): GEOLOGIC CROSS- SECTION (A-A').

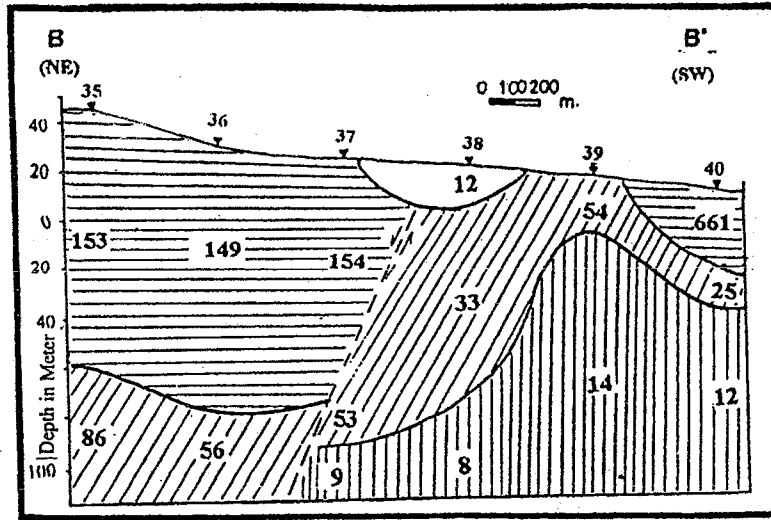


FIG.(16): ELECTRIC CROSS- SECTION (B-B').

Legend:

- 1st geo-electric layer.
- 2nd geo-electric layer.
- 3rd geo-electric layer.

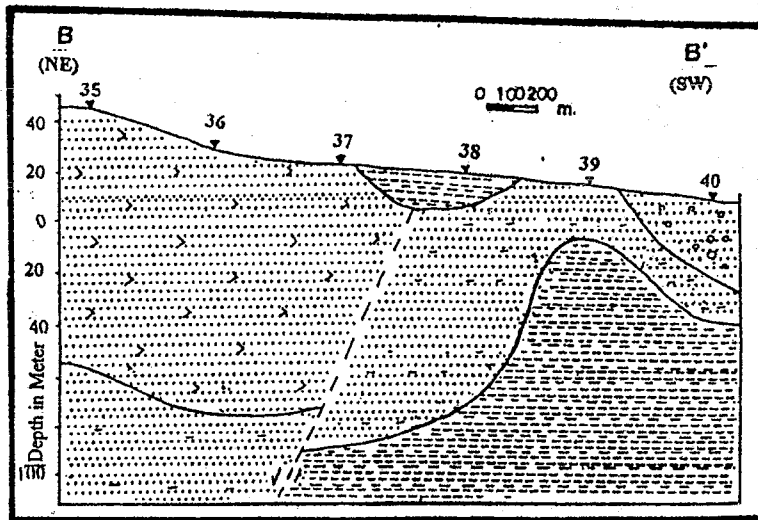


FIG.(17): GEOLOGIC CROSS- SECTION (B-B').

Legend:

- Limestone deposits (Pleistocene)
- Basic sands and gravels (Pleistocene)
- Sand interbedded with clay (Mid El-Nefous for. Pleocene)
- Clay (El-Mekhemus for. Mio. Pleocene)
- Deltic sand (El-Road for. L.Miocene)

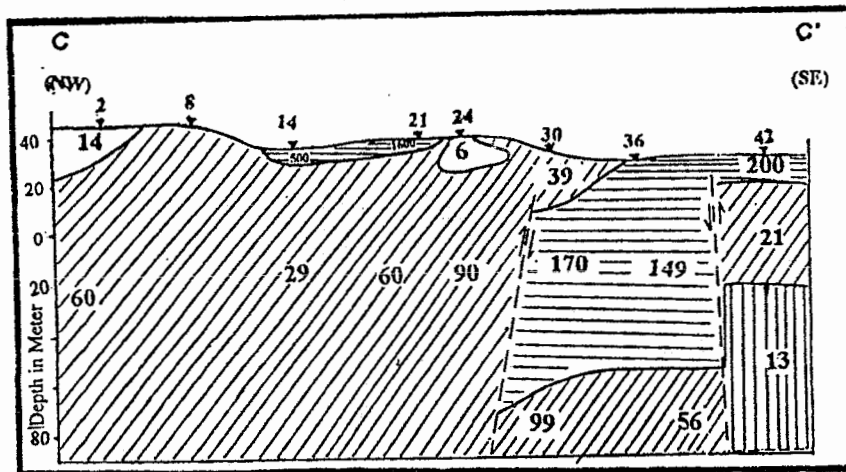


FIG.(18): ELECTRIC CROSS- SECTION (C-C').

Legend:

- 1st geo electric layer.
- 2nd geo electric layer.
- 3rd geo electric layer.

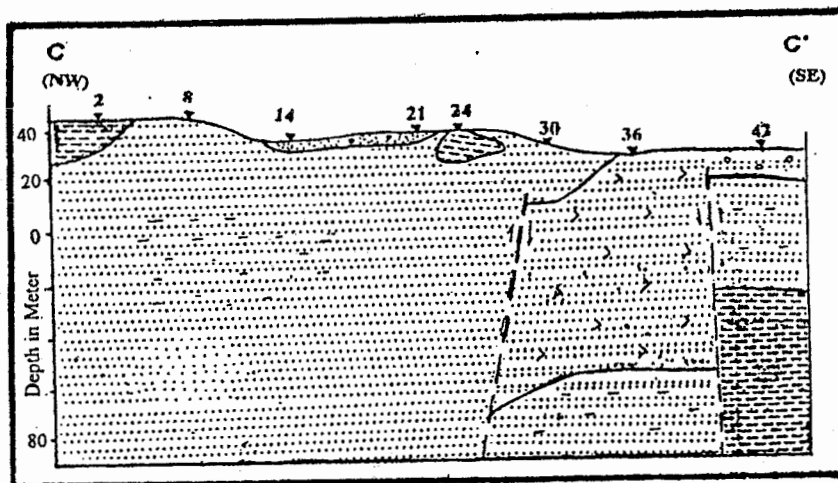


FIG.(19): GEOLOGIC CROSS- SECTION (C-C').

Legend:

- Luvuvulu deposits (F1-Miobocene)
- Nileitic sands and gravels (F1-Miobocene)
- Sand interbedded with clay (Wadi El-Natran Gr. Pliocene)
- Clay (El-Mekhlimes for. Mio. Pliocene)
- Detritic sand (El-Road for. I. Miocene)

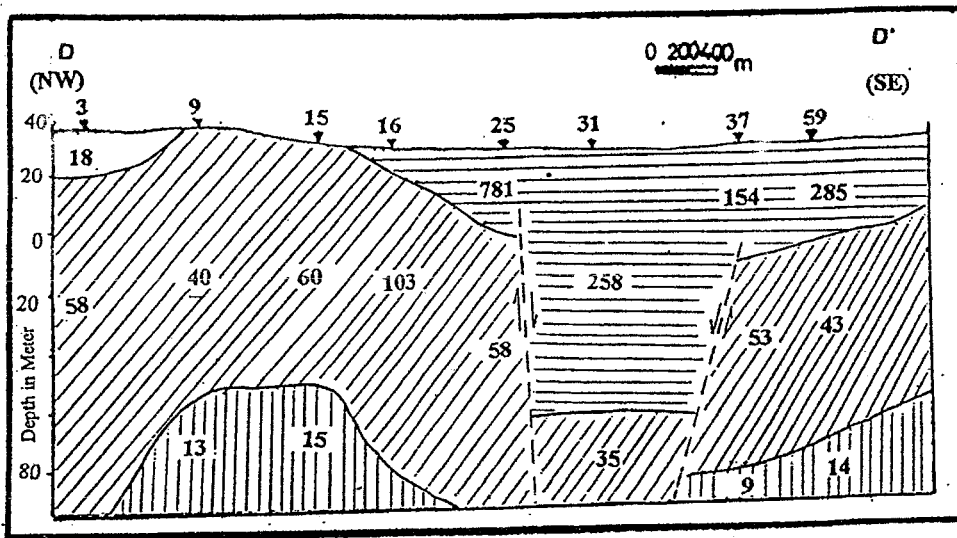


FIG.(20): ELECTRIC CROSS- SECTION (D-D').

Legend:
 □ 1st geo-electric layer. ▨ 2nd geo-electric layer. ▩ 3rd geo-electric layer.

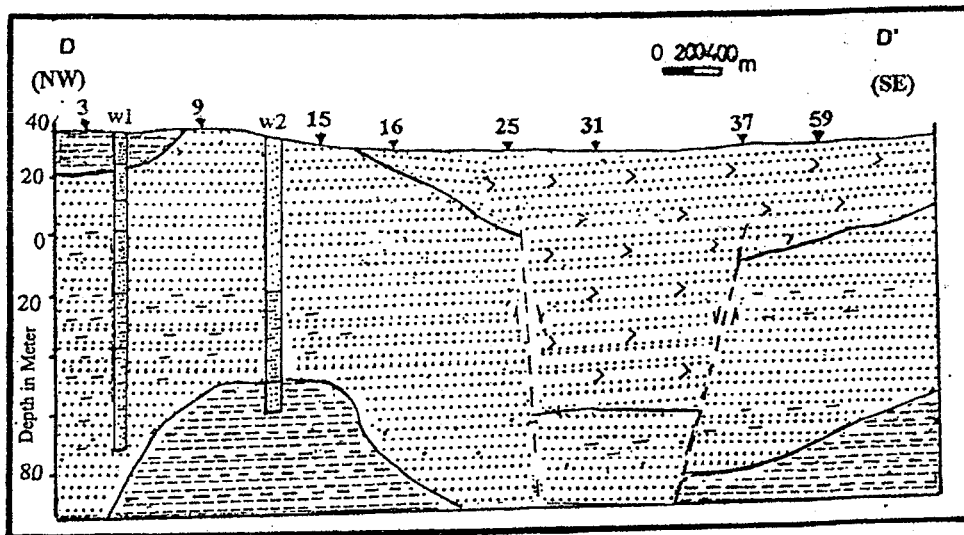


FIG.(21): GEOLOGIC CROSS- SECTION (D-D').

Legend:
 ▨ Lacustrine deposits (Pleistocene) ▩ Nileitic sands and gravels (Pleistocene)
 ▨ Sand interbedded with clay (Wadi El-Natrun for. Pliocene) ▩ Clay (El-Mokhles for. Mio. Pliocene)
 ▨ Detritic sand (F1-Rasel for. L.Miocene)

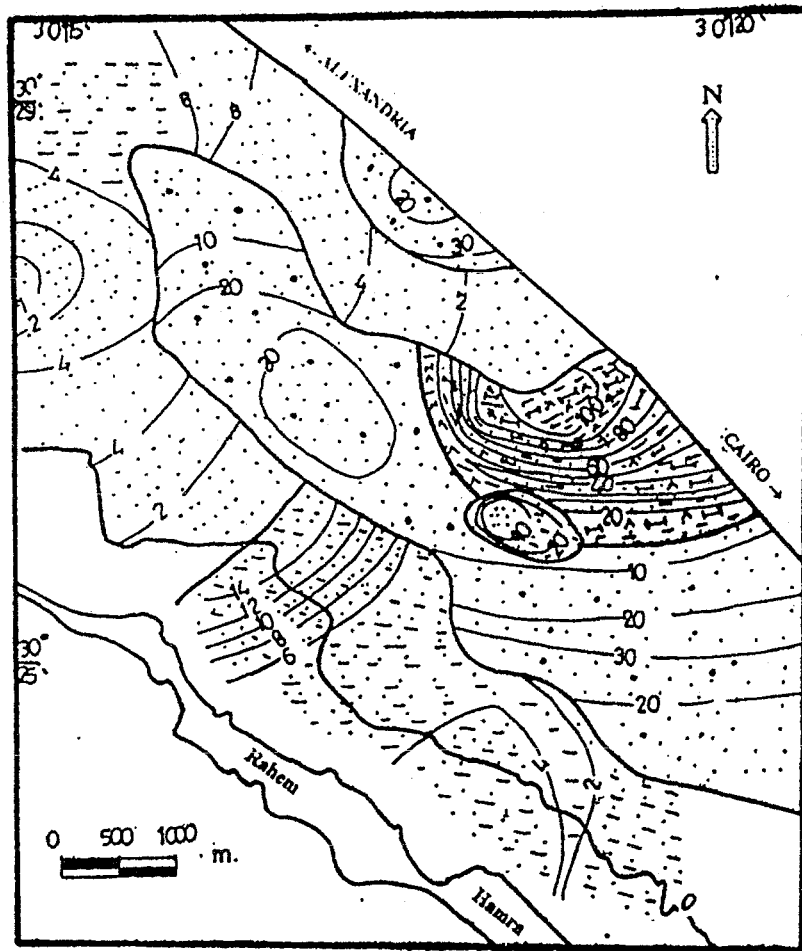






FIG.(22) : SOIL MAP OF THE STUDY AREA (BASED ON RESISTIVITY DATA).

-  Recent Sandes and Gravels
-  Loamy deposits
-  Acolian Sandes
-  Lake deposits (lacustrine)

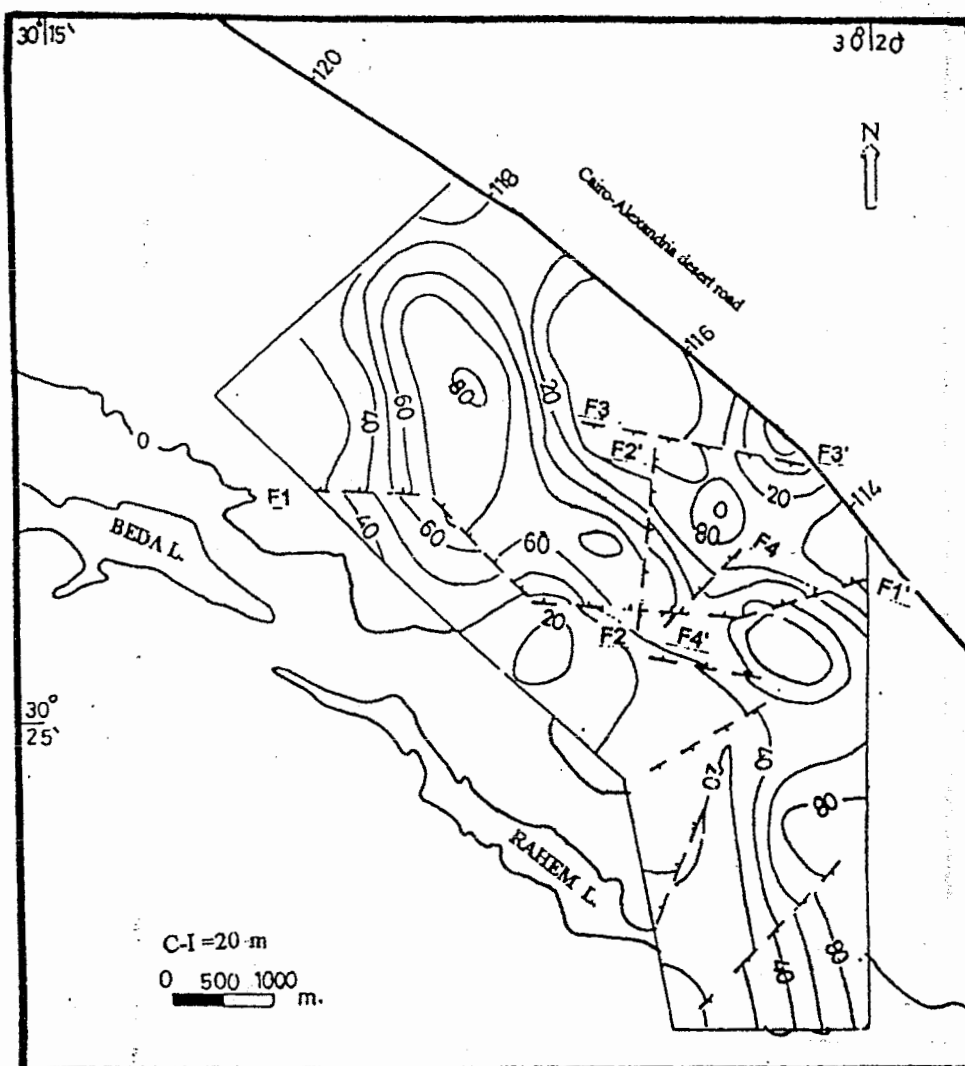


FIG.(23) : STRUCTURE CONTOUR MAP OF THE SURFACE OF THE MIO-PLIOCENE IMPERVIOUS CLAY BED.

A.,GH., HASSANEEN*, H.M., EL-SHAYEB** & M.,A., KHALIL*

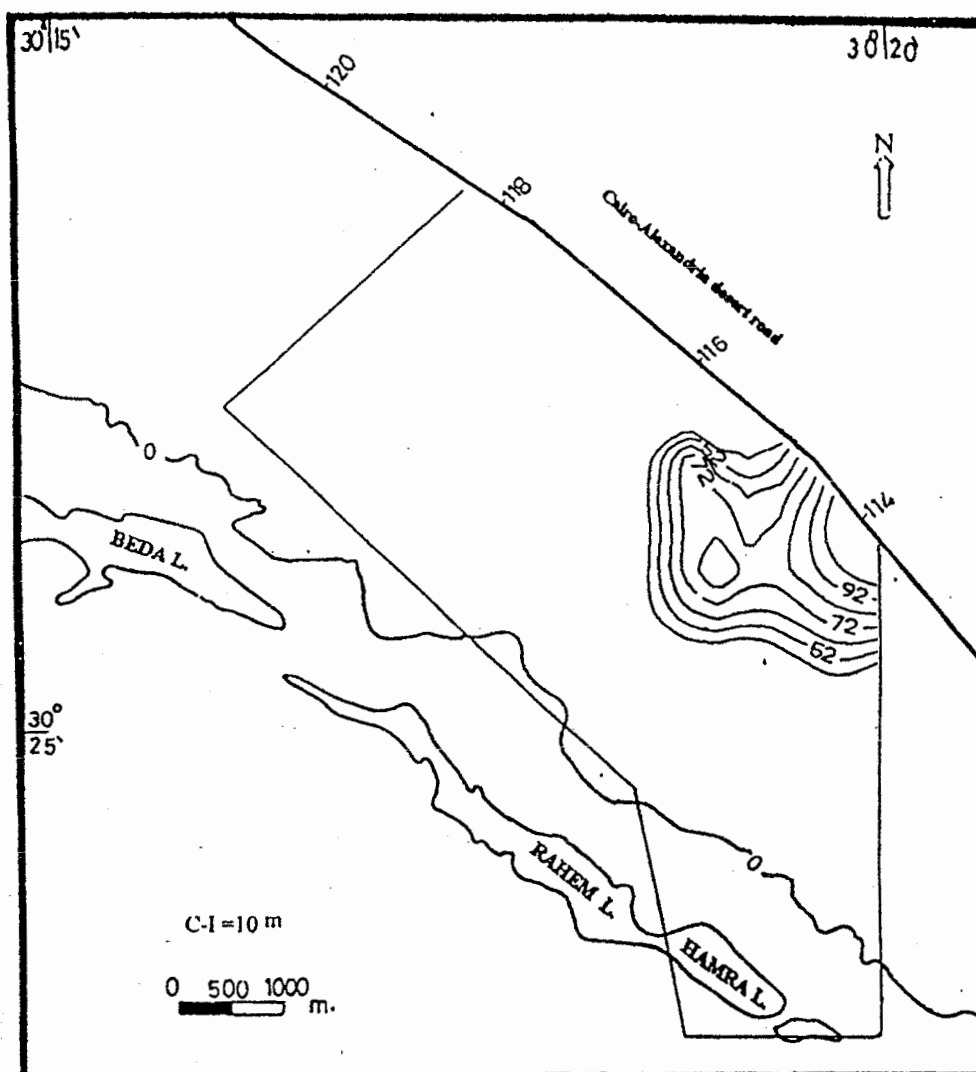


FIG.(24) : ISO-PACH MAP OF THE LACUSTRINE DEPOSITS.

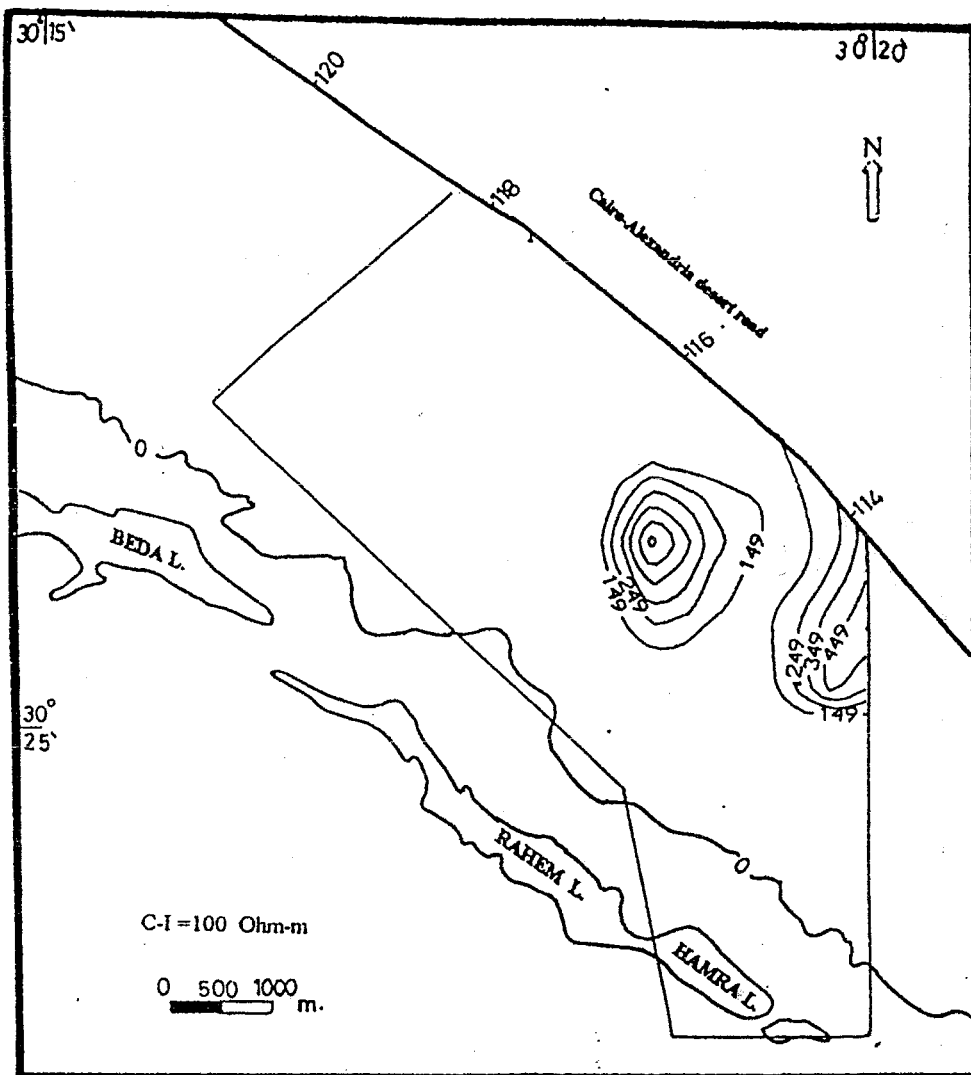


FIG.(25) : TRUE RESISTIVITY MAP OF THE LACUSTRINE DEPOSITS.

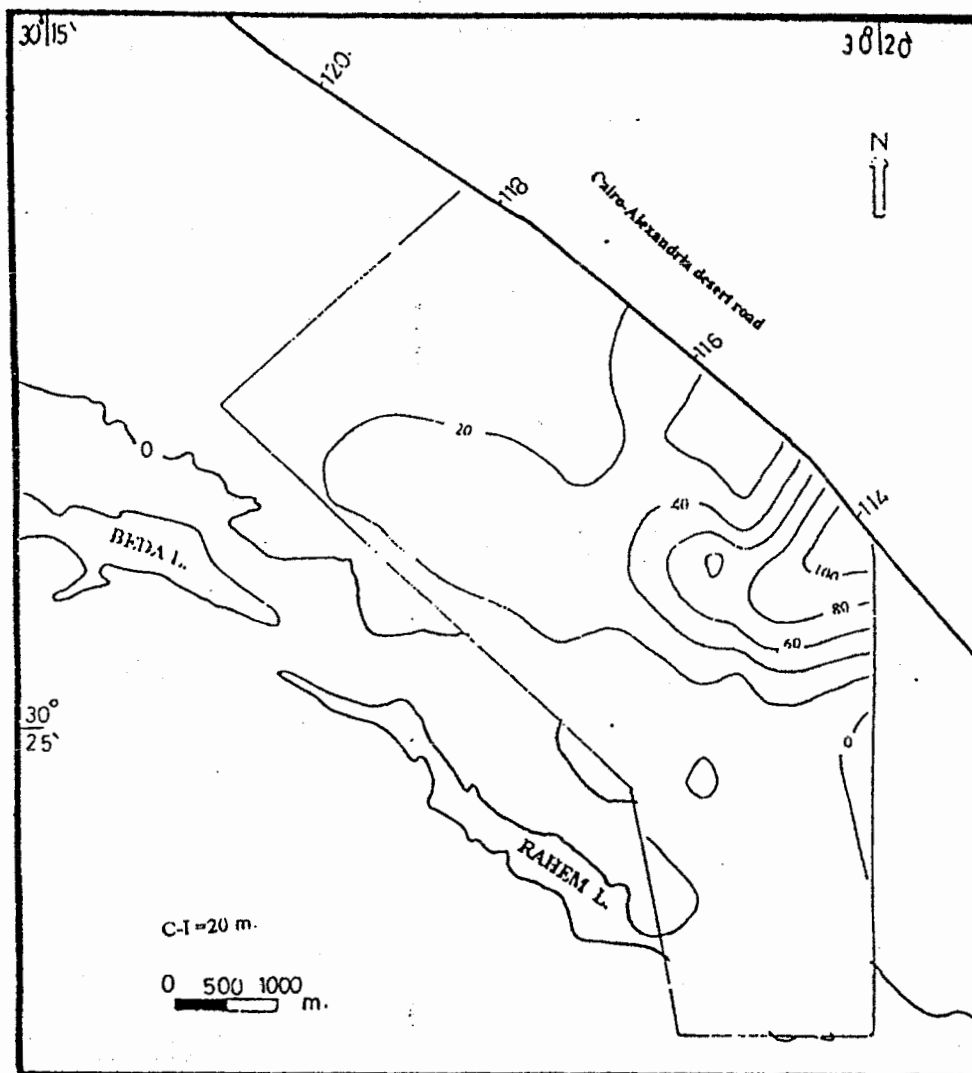


FIG.(26) : DEPTH TO WATER MAP OF THE PLIOCENE AQUIFER BASED ON RESISTIVITY DATA.

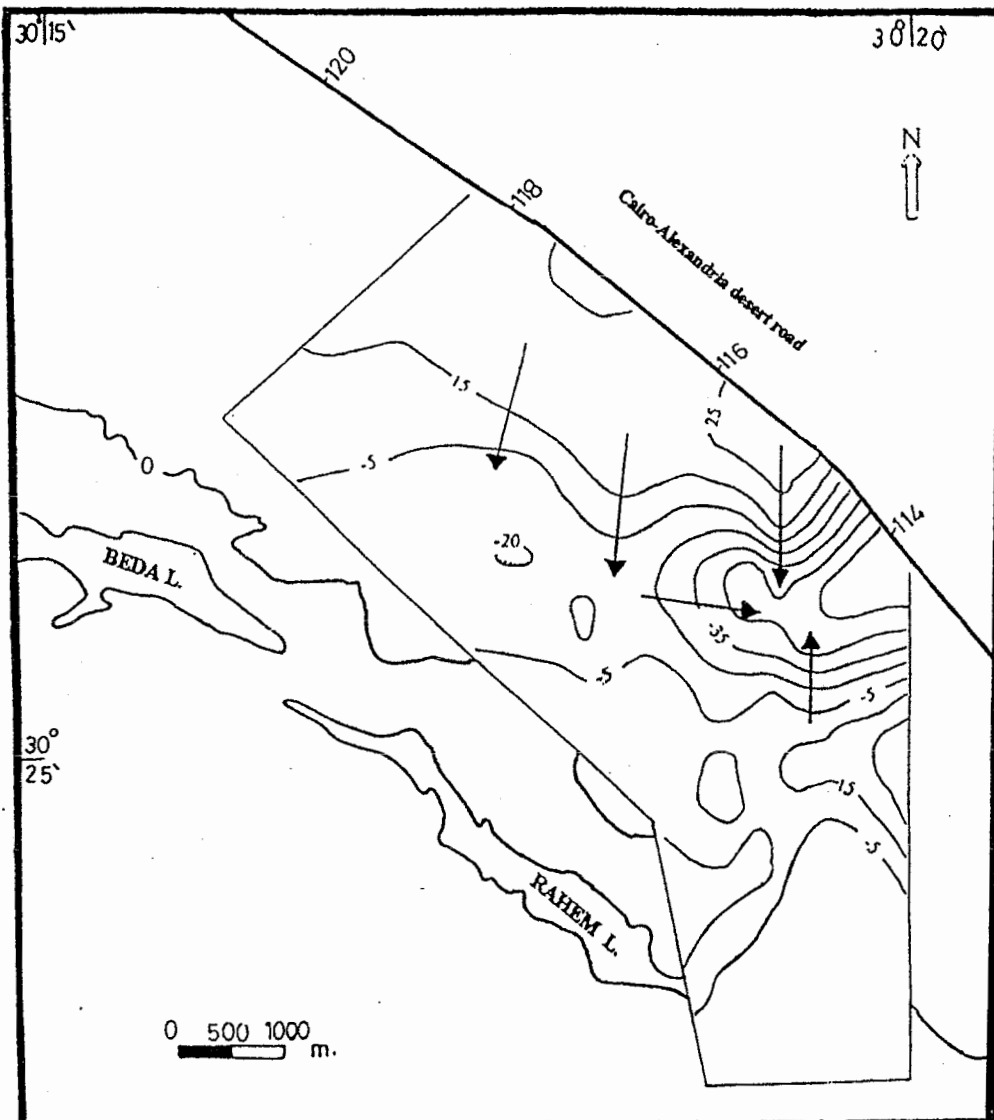


FIG.(27) : WATER TABLE MAP OF THE PLIOCENE AQUIFER
BASED ON RESISTIVITY DATA.

LEGEND:
— 3 — WATER TABLE CONTOUR LINE
→ DIRECTION OF GROUNDWATER FLOW.